



This is a repository copy of *Multibeam dual-circularly polarized reflectarray for connected and autonomous vehicles*.

White Rose Research Online URL for this paper:  
<http://eprints.whiterose.ac.uk/142636/>

Version: Accepted Version

---

**Article:**

Luo, Q., Gao, S., Li, W. et al. (6 more authors) (2019) Multibeam dual-circularly polarized reflectarray for connected and autonomous vehicles. IEEE Transactions on Vehicular Technology. ISSN 0018-9545

<https://doi.org/10.1109/tvt.2019.2897218>

---

© 2019 IEEE. Personal use of this material is permitted. Permission from IEEE must be obtained for all other users, including reprinting/ republishing this material for advertising or promotional purposes, creating new collective works for resale or redistribution to servers or lists, or reuse of any copyrighted components of this work in other works. Reproduced in accordance with the publisher's self-archiving policy.

**Reuse**

Items deposited in White Rose Research Online are protected by copyright, with all rights reserved unless indicated otherwise. They may be downloaded and/or printed for private study, or other acts as permitted by national copyright laws. The publisher or other rights holders may allow further reproduction and re-use of the full text version. This is indicated by the licence information on the White Rose Research Online record for the item.

**Takedown**

If you consider content in White Rose Research Online to be in breach of UK law, please notify us by emailing [eprints@whiterose.ac.uk](mailto:eprints@whiterose.ac.uk) including the URL of the record and the reason for the withdrawal request.



[eprints@whiterose.ac.uk](mailto:eprints@whiterose.ac.uk)  
<https://eprints.whiterose.ac.uk/>

# Multibeam Dual-Circularly Polarized Reflectarray for Connected and Autonomous Vehicles

Qi Luo, *Member, IEEE*, Steven Gao, *Senior Member, IEEE*, Wenting Li, Mohammed Sobhy, Ioanna Bakaimi, CH Kees de Groot, Brian Hayden, Ian Reaney, Xuexia Yang

**Abstract**—This paper presents a multibeam dual-circularly polarized (CP) reflectarray for connected and autonomous vehicles. The developed reflectarray uses one aperture to realize dual-band and multibeam operation. At each frequency band, there are two simultaneously shaped beams with different circular polarizations. Totally four beams are obtained with a single feed and each of the beams can be independently controlled. A simple but effective polarization suppression technique is introduced to suppress cross polarizations at large scan angles so the CP beam of the reflectarray can be configured to point at large angles. Thus, the present reflectarray is suitable to be applied to vehicles for reliable high data-rate satellite communications. To validate the design concept, an X-band prototype was designed, fabricated and measured. The design concept is flexible and can be applied to the design of dual-band, dual-CP reflectarray with different frequencies ratios. Moreover, the present design can also be extended to a continuous beam-steering design by incorporating phase shifters.

**Index Terms**—vehicles, Satcom-on-the-Move, circular polarization, reflectarray, multibeam, dual-band

## I. INTRODUCTION

CONNECTED and Autonomous Vehicle (CAV) is one of the most exciting technologies that will change the way how people and products are moved [1]. CAVs introduce many benefits, including reduction of crash rates and congestions, aiding mobility for disabled and older people [2], [3]. It is estimated that in the UK the market for CAVs will be worth 28bn in 2035 [4]. One of the key technologies for the success of the CAVs is reliable and high-speed communication system. Each CAV needs to communicate with the base stations, satellites and other vehicles. For example, dedicated

short-range communications (DSRC) are developed to enable fast and secure vehicle-to-vehicle and vehicle-to-infrastructure communication [5]. Intelligent transportation system (ITS) is developed to provide safer and more coordinated transport networks [6]. Satellite communication has inherent advantages such as being more robust and secure, as well as having better coverage in rural areas. Thus, besides providing the navigation services to the vehicles, satellite communications will be the key technology to support CAVs. Satellite telecommunications companies such as Intelsat and Inmarsat are working on satellite powered connectivity solutions for the connected cars.

Fig. 1 shows the different communication links for the CAVs. To communicate with the roadside unit (RSU), moderate gain antennas with wide beamwidth are used for the purpose of better coverage [7]. Wideband antennas with broad beamwidth are used for car-to-car communication [8], [9]. Regarding the broadband satellite data service such as the direct-broadcast-satellite service, it is desirable to have high gain and circularly polarized (CP) antennas with wide beam scanning angles. An array antenna with wide beam scanning angle enables vehicles to keep track of the satellites so it is always within the reception area of the satellite and does not fall in the blind spot. The traditional approach to obtaining a high gain CP antenna is to use the phased array or reflector antenna [10]. Although the phased array has a planar configuration, it requires sophisticated beamforming network (BFN) especially when the number of antenna elements is large, which leads to a high-cost. Moreover, obtaining large angle beam scanning of the CP phased array is challenging due to the reason that the radiating elements normally have narrow CP beamwidths (e.g.  $\pm 30^\circ$ ). Although some wide beamwidth circularly polarized antenna elements were reported [11], they are not suitable for the design of planar array antennas. On the other hand, the reflector antenna can provide beam scanning through mechanically rotating the antenna. Yet, the reflector antenna has a high profile and has high mass.

Reflectarray antennas have attracted much research interests in recent years and have already been applied to automotive radars [12]. They combine the advantages of the reflector antenna and the phased array [13]. A reflectarray antenna normally consists of planar radiating elements and at least one feed antenna. To reduce the profile, folded configuration [12], [14] can be used. The reflectarray use space-fed technique to excite the antenna elements, thus avoiding the use of the feed network. Therefore, the reflectarray is a good candidate for the design of affordable and lightweight satellite antenna system of the CAVs. Although there are many studies [15], [16] on

Copyright ©2015 IEEE. Personal use of this material is permitted. However, permission to use this material for any other purposes must be obtained from the IEEE by sending a request to pubs-permissions@ieee.org.

Qi Luo, Steven Gao, Wenting Li and Mohammed Sobhy are with the Department of Engineering and Digital Arts, University of Kent, Canterbury, CT2 7NZ UK e-mail: (qiluo@ieee.org; s.gao@kent.ac.uk; M.I.Sobhy@kent.ac.uk). This work was supported by the EPSRC Project under Grant EP/N032497/1 and EP/P015840/1.

Ioanna Bakaimi and Brian Hayden are with Chemistry Faculty, University of Southampton, Southampton, SO17 1BJ UK e-mail: (I.Bakaimi@soton.ac.uk; B.E.Hayden@soton.ac.uk)

CH Kees de Groot is with Faculty of Physical Sciences and Engineering, University of Southampton, Southampton, SO17 1BJ UK e-mail: chdg@ecs.soton.ac.uk

Ian Reaney is with Department of Materials Science and Engineering, University of Sheffield, Southampton, S1 3JD UK e-mail: i.m.reaney@sheffield.ac.uk

Xue-Xia Yang is with the Key laboratory of Specialty Fiber Optics and Optical Access Networks, Shanghai Institute of Advanced Communication and Data Science, Joint International Research Laboratory of Specialty Fiber Optics and Advanced Communication, Shanghai University, China (yang.xx@shu.edu.cn).

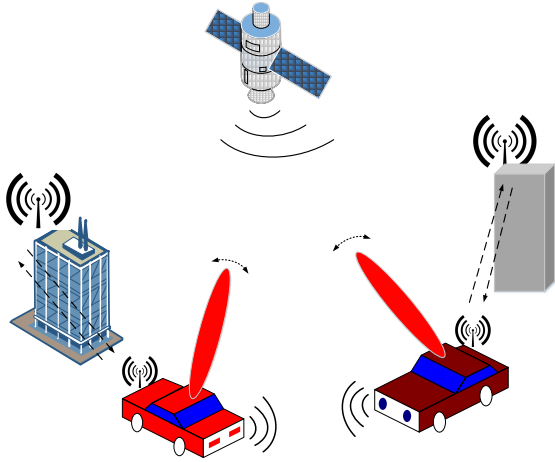


Fig. 1. Demonstration of the different communication links for the CAVs.

improving the maximum beam steering angle of linearly polarized array antennas, to date, there are few reported researches on the CP array antenna with large scan angles. Recent study shows that through using a frequency scanning leaky-wave antenna [17], circularly polarized beam scanning range from  $-40^\circ$  to  $25^\circ$  can be obtained. Dual-CP reflectarray has also received increasing research interests. Although dual-CP reflectarrays can be realized by using elements with variable rotation angles [18] or using CP selective surfaces [19], there are few reports on the single aperture dual-CP reflectarrays that can generate simultaneous beams with orthogonal CPs and the beams can be independently controlled. In [20], a dual-CP reflectarray is obtained by using a dual-surface reflector and polarizer which converts the LP waves to CP waves. One dual-CP reflectarray that can steer its beam to  $21^\circ$  with independent control was reported in [21]. In this design, Dual-CP operation was achieved by placing one left-hand circular polarization (LHCP) and one right-hand circular polarization (RHCP) selective surfaces at different layers separated by an air gap, which results in a complicated structure and high profile.

In this paper, a novel dual-band reflectarray antenna with dual-circular polarizations and independent beam control is developed. Within each frequency band, there are two shaped beams, one for left-hand and one for right-hand circular polarization. Thus, four simultaneously focused beams are achieved for each feed. Moreover, the frequency ratio of the dual-band operation is flexible and the central frequency of each band can be designed independently. This allows the developed antenna suitable for the multiple-input-multiple-output (MIMO) communications for vehicles by taking advantages of the polarization and frequency diversity [22], [23]. In this way, the CAVs can always keep reliable links with the satellites and important information such as enhanced mapping, navigational data, over-the-air software and firmware updates can be received in time. A simple but effective cross-polarization suppression technique is developed to improve beam scanning performance of the present reflectarray. This technique does not increase the system complexity and can ef-

fectively suppress the cross polarizations so the array antenna can maintain good CP radiations at large scan angles. Fig. 2 show the concept of the multibeam dual-CP reflectarray on the vehicles.

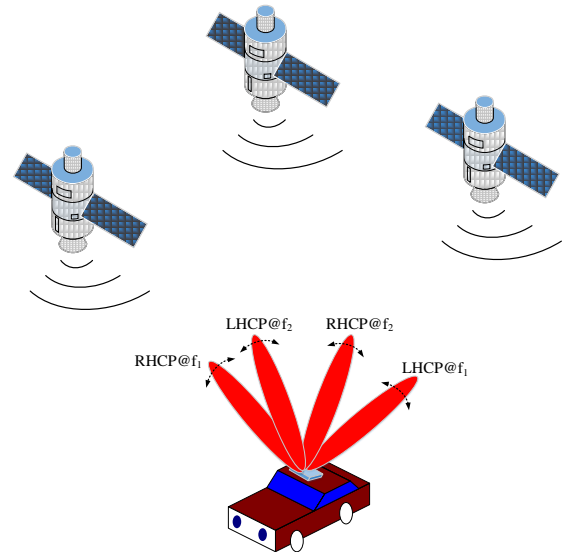


Fig. 2. Concept of the dual-band, dual-CP reflectarray on the vehicles.

This paper is organized as follows. Section II details the design of the reflectarray unit cells. Section III presents the design and analysis of the dual-band, dual-CP reflectarray, as well as the cross polarization suppression technique. The simulation and measurement results of the prototypes including the simulation of the present antenna on the roof of the vehicle are given in Section IV. Section V concludes the paper.

## II. DESIGN OF THE REFLECTARRAY UNIT CELL

### A. Unit Cell Configuration

Fig. 3 shows the configuration of the reflectarray unit cell. Two equilateral triangular patches of different sizes are positioned in a parallelogram with one of the patches rotated by  $180^\circ$ . One resonates at the higher frequency and the other resonates at the lower frequency. Using this configuration, the unit cell can be used to form a dual-band interleaved array antenna with a triangular lattice. The length of the equilateral triangular patch is calculated by using the formula given in [24]:

$$f_{mn} = \frac{2c}{3a\epsilon_r^{1/2}}(m^2 + mn + n^2)^{1/2} \quad (1)$$

where  $c$  is the speed of light,  $a$  is the side length of the equilateral triangular patch,  $\epsilon_r$  is the relative dielectric permittivity of the substrate and  $mn$  refers to the  $TM_{mn}$  modes. Each of the triangular patches is fed by two proximity microstrip lines of  $50\Omega$  characteristic impedance. CP radiation is obtained by feeding the patch with  $90^\circ$  phase difference. The feed lines are electromagnetically coupled to a branch line coupler through a rectangular aperture etched on the ground plane below the feed lines. The four ports of the coupler are terminated with  $50\Omega$  microstrip lines. The width of the feed lines is calculated by using the formulas given in [25].

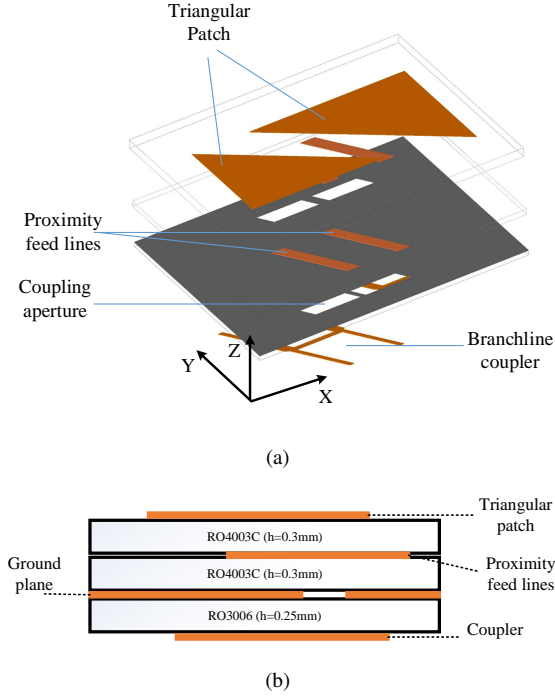


Fig. 3. (a) Exploded and (b) side view of the unit cell of the proposed reflectarray.

Because the feed lines are electromagnetically coupled, there is no need for using any vias, thus the fabrication complexity and cost for the reflectarray antenna design are significantly reduced. To verify the design concept, it was decided to design an X-band reflectarray prototype. Two frequencies within X-band were selected, 8.6 GHz and 10.1 GHz, representing a frequency ratio of 1.17. It should be noted that a small frequency ratio is chosen in this study for the purpose of configuring the beam of the array to large angles without the appearance of grating lobes at both frequencies. The size of the patch can be independently adjusted to operate at different frequencies (different frequency ratio). The only constraint is the required grating lobes free beam steering angles. As shown in Fig. 3 (b), the antenna element has four conductive layers and three dielectric layers. The radiating elements and the feed lines are printed on separate RO4003C substrates ( $\epsilon_r = 3.55$ ,  $\tan \sigma = 0.0027$ ) with a thickness of 0.3 mm. In order to keep the compact size of the branch line couplers, they are printed on a higher permittivity substrate, 0.25 mm thick RO3006 substrate ( $\epsilon_r = 6.15$ ,  $\tan \sigma = 0.002$ ).

### B. Simulation results

The mutual coupling between the elements can change the input impedance and shift the resonant frequency of the antenna element. Thus, it is necessary to simulate the unit cell of the reflectarray with periodic boundaries in order to take into account the mutual coupling between adjacent elements, and then perform some optimizations. The optimizations include changing the position of the proximity feed lines and slightly changing the size of the patches to overcome the effects caused by the mutual couplings. Good impedance matching is critical

for this design because poor impedance matching degrades the isolation between each polarization. After optimization, the side length of the higher band and lower band patches are chosen to be 10.9 mm and 13 mm, respectively. Fig. 4 shows the values of the key dimensions of the CP equilateral triangular patches.

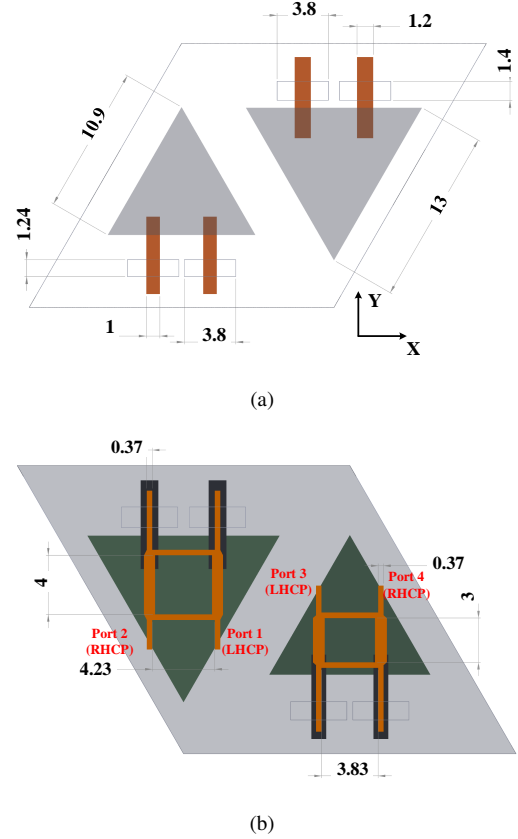
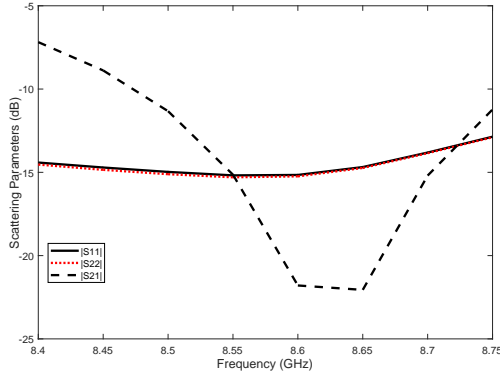


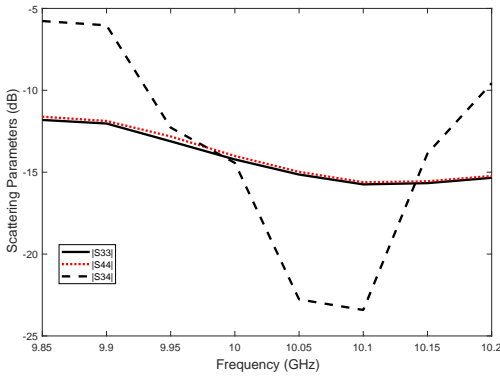
Fig. 4. The dimensions (in millimetre) of the X-band design (a) Radiating element, feed lines and coupling slots (b) branch line coupler.

Fig. 5 shows the simulated scattering parameter of radiating element 1 (lower band antenna) and radiating element 2 (higher band antenna). The port numbers are shown in Fig. 4 (b). The simulation results show that at the resonant frequencies of the two patches, the isolation is always higher than 20 dB while the return loss is better than 15 dB. Fig. 6 shows the simulated axial ratio of the unit cell. As shown, the unit cell has low axial ratios at both resonant frequencies. Within the impedance bandwidth of the patches, the axial ratio is always smaller than 3 dB.

Microstrip delay lines are connected to the input ports of the couplers to provide the required phase delays in order to form the shaped beams. There are two groups of phase delay lines for each coupler, one for LHCP radiation and another for RHCP radiation. As a result, there are four groups, each group of the phase delay lines corresponds to the phase distribution of one beam. Because these four sets of phase distribution can be defined independently and changing one set of the phase distribution has little effect on the others, these four beams can be independently controlled. The phase delay lines are designed to provide phase delays up to  $360^\circ$ . Fig. 7



(a)



(b)

Fig. 5. Simulated scattering parameter of (a) radiating element 1 and (b) radiating element 2 using Floquet port.

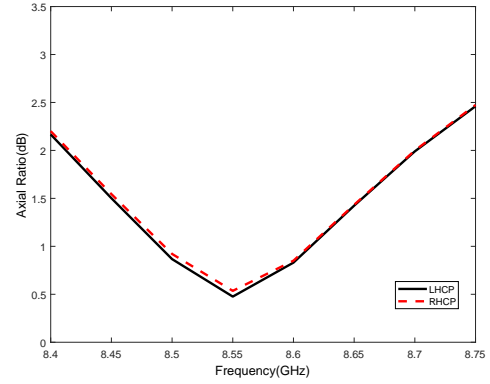
shows the simulated reflection phase and amplitude of the unit cell at 8.6 GHz and 10.1 GHz. As shown, the phase variation is linear when the total length of the microstrip delay line increases. The insertion loss of unit cell is about 1.5 dB at both resonant frequencies. Besides the loss of the element itself, the insertion loss of the coupler introduces approximately 0.2 dB loss. Another insertion loss is from the coupled line. As shown in Fig. 3 (b), to avoid the using of vias, the coupler and the phase delay lines of the patch antenna are electromagnetically coupled, which introduces around 0.4 dB loss.

### III. DESIGN OF THE REFLECTARRAY

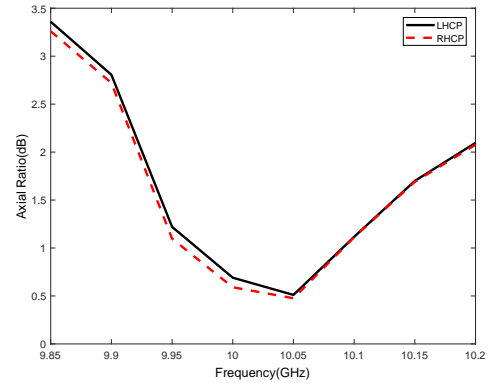
#### A. Array configuration

Fig. 8 shows two types of reflectarray configuration that can be used for the vehicle application, considering that the antenna would be mounted on the roof of the car. One is center-fed and the other is offset-fed. Both configurations can be realized using the same design principle. In this study, the center-fed configuration is used, for the purpose of simplifying the prototype fabrication and characterization.

Fig. 9 shows the top and back view of the designed reflectarray antenna. As shown, two planar array antennas are interleaved in the same aperture which has a diameter of 234 mm. Each of the array antennas has 75 radiating elements positioned in a triangular lattice with a separation



(a)



(b)

Fig. 6. Simulated axial ratio of the unit cell: (a) 8.6GHz band and (b) 10.1GHz band.

distance of 22.5 mm ( $0.64\lambda_{8.6GHz}$  and  $0.75\lambda_{10.1GHz}$ ). With this distance, in theory, the beam can be steered to  $\pm 55^\circ$  at the lower resonant frequency without any grating lobes. Two feeds are used for the reflectarray to validate the beam-switching performance and the largest beam-switching angle of the reflectarray. The positions of the feeds are defined by considering the CP beamwidth of the feed, to ensure that most of the radiating elements are illuminated by the CP waves radiated from the feed. In this design, the distance between the horn antenna and the reflectarray panel is chosen to be 135mm above the center of the planar array. An X-band dual-CP septum horn antenna that operates from 8 to 12 GHz is designed to be used as the feed of the reflectarray. The septum was designed by using the method given in [26].

#### B. Cross polarization suppression technique to improve the beam-scanning performance

It is always a design challenge to steer the beam of a CP array antenna to large angles. Besides the increased mismatching and scan loss, which are problems experienced by the LP array antennas, the CP arrays also face the degradation of the axial ratio due to the increase of the cross polarization. In this study, an effective cross polarization suppression technique is developed to improve the beam-scanning performance of the dual-CP reflectarray. When the present reflectarray operates in

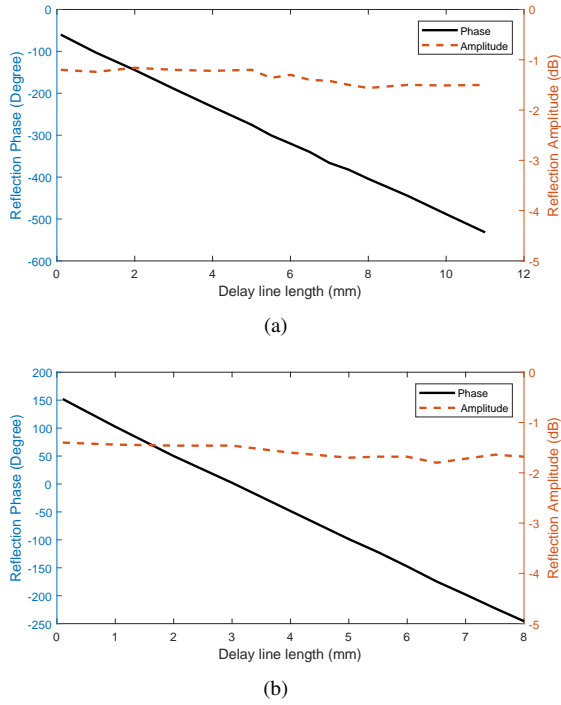


Fig. 7. Simulated reflection phase and amplitude of the unit cell at (a) 8.6GHz and (b) 10.1GHz.

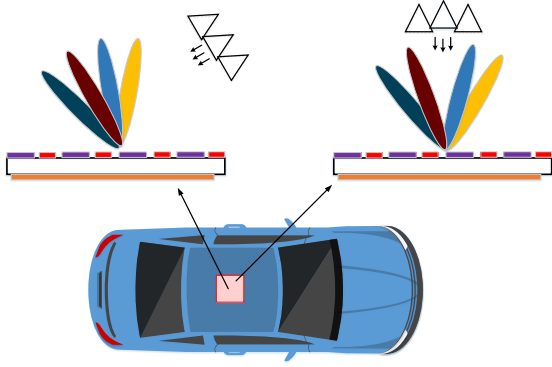


Fig. 8. Reflectarray with center-fed and offset-fed configuration on the car roof.

the LHCP mode, its electrical field in the far-field region is expressed as

$$\vec{E}_{total}(\theta, f) = \vec{E}_{t,LHCP}(\theta, f) + \vec{E}_{t,RHCP}(\theta, f) \quad (2)$$

where  $\vec{E}_{t,LHCP}(\theta, f)$  and  $\vec{E}_{t,RHCP}(\theta, f)$  are the total electrical field of the LHCP and RHCP waves, respectively. The cross polarization components are composed of three sources

$$\vec{E}_{t,RHCP}(\theta, f) = \vec{E}_{patch,RHCP}(\theta, f) + \vec{E}_{feed,RHCP}(\theta, f) + \vec{E}_{coupler,RHCP}(\theta, f) \quad (3)$$

where  $\vec{E}_{patch,RHCP}(\theta, f)$  is the cross-polarization of the patch antenna,  $\vec{E}_{feed,RHCP}(\theta, f)$  is the cross-polarization of the feed antenna and  $\vec{E}_{coupler,RHCP}(\theta, f)$  is the re-reflected signal from the RHCP port of the coupler.

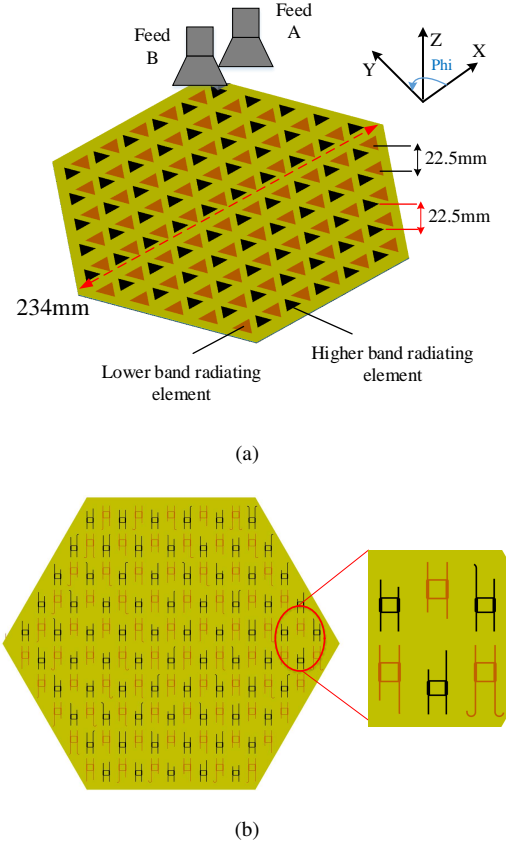


Fig. 9. (a) Top view and (b) back view of the present reflectarray antenna.

Because the feed antenna has high polarization purity, its cross-polarization can be ignored and Eq.3 is simplified to

$$\vec{E}_{t,RHCP}(\theta, f) \approx \vec{E}_{patch,RHCP}(\theta, f) + \vec{E}_{coupler,RHCP}(\theta, f) \quad (4)$$

Since the amplitude of these two components are similar, from Eq. 4, it can be concluded that if at any radiating element these two components are out of phase as shown in Fig. 10, then the RHCP radiation can be suppressed.

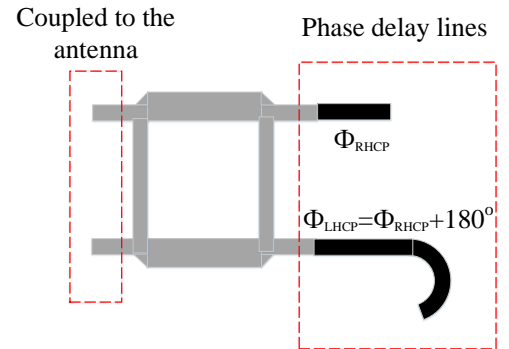


Fig. 10. The ideal phase differences between the LHCP and RHCP phase delay lines.

The required phase differences can be realized by introducing an additional reference phase when calculating the required

phase for each radiating element

$$\phi_R = k_0(d_i - (x_i \cos \varphi_b + y_i \sin \varphi_b) \sin \theta_b) + \Delta ph \quad (5)$$

where  $\phi_R$  is the phase of the reflection coefficient of the antenna element  $i$ ,  $k_0$  is the phase constant in vacuum,  $(x_i, y_i)$  are the coordinates of the array element  $i$ ,  $d_i$  is the distance from the phase centre of the feed to the antenna unit cell,  $(\theta_b, \varphi_b)$  are the expected scan angles of the beam in spherical coordinates and  $\Delta ph$  is the additional reference phase. It is shown in [27] that the bandwidth of the reflectarray can be improved by introducing this additional reference phase, but in this study, the additional reference phase is used to suppress the cross polarization components of the reflectarray.

In this work, the reflectarray has simultaneous dual-CP beams at different scan angles, which means it is impossible to maintain the exact 180 degree phase differences at each radiating element. Instead, in order to maximize the cross polarization suppression effect,  $\Delta ph$  should be calculated as an averaged value

$$\Delta ph = \frac{\sum_{n=1}^N w_n (\phi_{n,LHCP} - \phi_{n,RHCP} + 180^\circ)}{N} \quad (6)$$

where  $N$  is the total number of the radiating elements,  $\phi_{n,LHCP}$  is the required phase for antenna element  $n$  to have a LHCP focused beam and  $\phi_{n,RHCP}$  is the required phase for antenna element  $n$  to have a RHCP focused beam. In this equation,  $w_n$  is the weight coefficient and it should have larger values for the central radiating elements (where they have higher amplitudes) and the smallest value for the radiating elements in the edge (where they have the smallest amplitudes). As an example, Fig. 11 shows the weights used in this study.

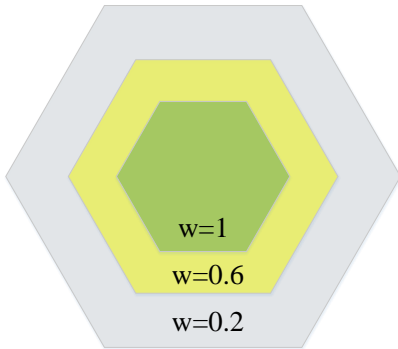
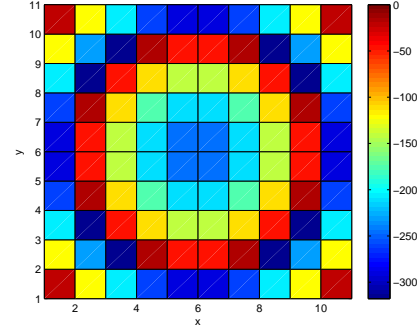


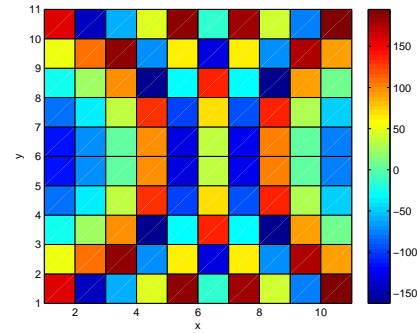
Fig. 11. The weight coefficient used for the present reflectarray when calculating the additional reference phase.

Fig.12 (a) shows the calculated phase distribution at 8.6 GHz to have the LHCP beam at broadside ( $\theta = 0^\circ$ ), and Fig.12 (b) shows the calculated phase distribution at 8.6 GHz to have the RHCP beam at  $\theta = -45^\circ$  after adding the additional reference phase calculated by using Eq.6. It is found that after applying the developed method, most of the radiating elements have a phase difference within the range of  $180^\circ \pm 60^\circ$  between their LHCP and RHCP phase delay lines. Thus, conjugate field matching is achieved and the cross-polarization components are suppressed, which improves the polarization purity of the

circularly polarized reflectarray. Applying this technique to the present dual-CP reflectarray, the beam-scanning range of the reflectarray is increased to larger angles. As will be presented in the next section, the maximum beam scanning angle of the reflectarray is improved to  $-55^\circ$  at 8.6 GHz.



(a)



(b)

Fig. 12. Calculated phase distribution of the reflectarray to have (a) a focused LHCP beam at  $\theta = 0^\circ$  and (b) a focused RHCP beam at  $\theta = -45^\circ$ .

#### IV. EXPERIMENTAL AND SIMULATION RESULTS

A prototype of the designed reflectarray was fabricated and measured. There are 75 radiating elements for higher and lower band operation respectively. These triangular patches are interleaved and placed in a hexagonally shaped aperture with a diameter of 234 mm. It should be noted that the size of the antenna was chosen considering the fabrication limitation on the PCB size in the University workshop. For practical applications, the requirements on the directivity of the array can be reached by choosing the appropriate aperture size of the array antenna. The resonant frequency is determined by the size of the triangular patch and can be re-sized in order to obtain different resonant frequencies. To validate the beam scanning performance of the dual-CP multi-beam reflectarray, two feeds were used. Feed A is the one positioned above the centre of the reflectarray while Feed B is offset by 22.5mm in X-axis (see Fig. 9). Because the prototype is a passive design, in order to verify the largest CP beam steering angles that can be achieved, the phase distribution of the reflectarray is defined to have the fixed beams pointing at its largest theoretical angles.

Fig. 13 (a)-(d) show the measured and simulated radiation patterns when Feed A is excited. The beams are all defined in  $\phi = 0$  plane and the coordinates are given in Fig. 9. During the measurement, when one feed is excited, the other feed is terminated with a matched load. In general, there is good agreement between the measurement and simulation results in the aspect of beam-steering. The measurement results show higher side lobes and wider beamwidth, which are mainly caused by the phase errors from fabrication inaccuracy, the reflections from the RF connectors, the mounting structure of the feed horn as well as the coaxial cables. Because the designed reflectarray has a multilayer configuration and the phase delay lines are excited by electromagnetic coupling, so the alignment accuracy is the main source of the phase errors. Moreover, during the measurement, one port of the dual-CP horn is terminated by a broadband load, which also caused some unavoidable reflections.

Fig. 14 (a)-(d) show the measured and simulated radiation patterns when Feed B is excited. This measurement is used to evaluate the beam scanning performance of the designed reflectarray. It is shown that at 10 GHz the angles of the beams are switched to  $-18^\circ$  and  $-38^\circ$  for the RHCP and LHCP beams, respectively. For the RHCP and LHCP beams at 8.6 GHz, the angles of the beams are switched to  $-55^\circ$  and  $-7^\circ$ , respectively. All of these beams show low cross polarizations. Table I summarizes the beam angles of the reflectarray when Feed A or Feed B is active.

To further validate the developed cross-polarization suppression technique, a reference design that removes the phase delay lines of the LHCP port of the 8.6 GHz antenna elements was designed and simulated. In this case, there is no cross-polarization suppression from the LHCP radiation to RHCP radiation. Meanwhile, the theoretical radiation pattern of the reflectarray which assumes that the triangular patch is RHCP polarized was also calculated using the array theory. These results are compared in Fig. 15. Both simulated and calculated results confirm that without applying the cross polarization suppression technique, there is high cross polarization at large scan angles which degrades the CP performance of the reflectarray.

Fig. 16 shows the measured gain variation of the present reflectarray at different scan angles. As shown, at 10.1GHz when the beam is steered to  $-38^\circ$ , the gain variation is less than 3.5 dB. At 8.6 GHz, when the beam is steered to the  $-55^\circ$ , the gain variation is about 3 dB.

TABLE I  
BEAM ANGLES OF THE FABRICATED PROTOTYPES WITH FEED A AND FEED B EXCITED.

	Feed A active	Feed B active
RHCP@10GHz (Beam 1)	$\theta = -8^\circ, \phi = 0^\circ$	$\theta = -18^\circ, \phi = 0^\circ$
LHCP@10GHz (Beam 2)	$\theta = -30^\circ, \phi = 0^\circ$	$\theta = -38^\circ, \phi = 0^\circ$
RHCP@8.6GHz (Beam 3)	$\theta = -45^\circ, \phi = 0^\circ$	$\theta = -55^\circ, \phi = 0^\circ$
LHCP@8.6GHz (Beam 4)	$\theta = 0^\circ, \phi = 0^\circ$	$\theta = -7^\circ, \phi = 0^\circ$

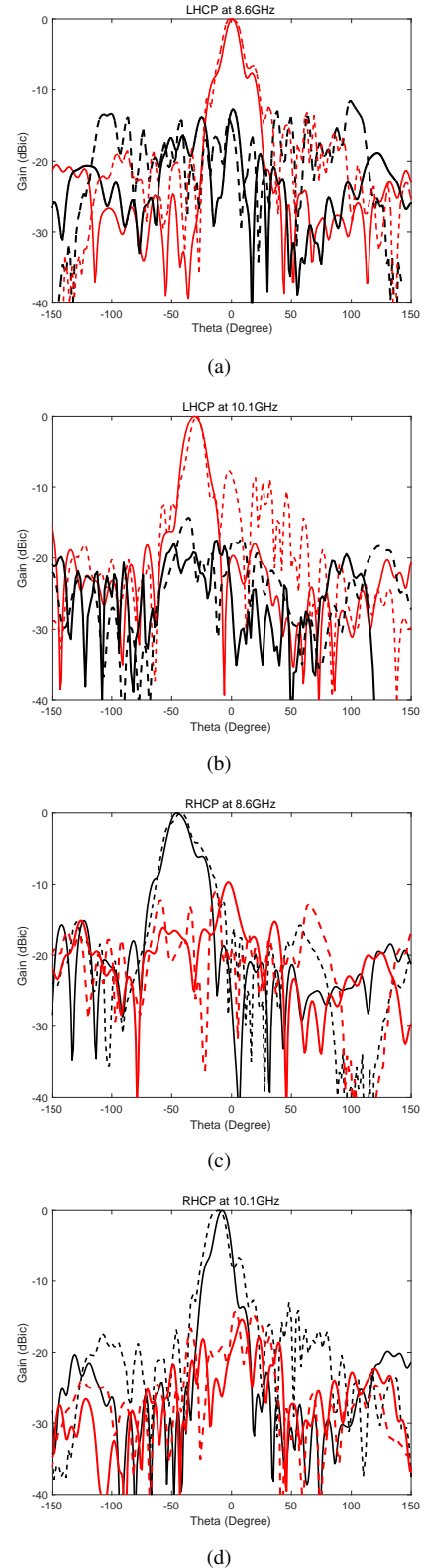


Fig. 13. Simulated and measured radiations patterns when Feed A is excited: (a) LHCP beams at 8.6GHz; (b) LHCP beams at 10.1GHz; (c) RHCP beams at 8.6GHz; (d) RHCP beams at 10.1GHz. (Black solid line: simulated RHCP, Black dashed line: measured RHCP, Red solid line: simulated LHCP, Red dashed line: measured LHCP)

Fig. 17 shows the simulated radiation patterns of the devel-

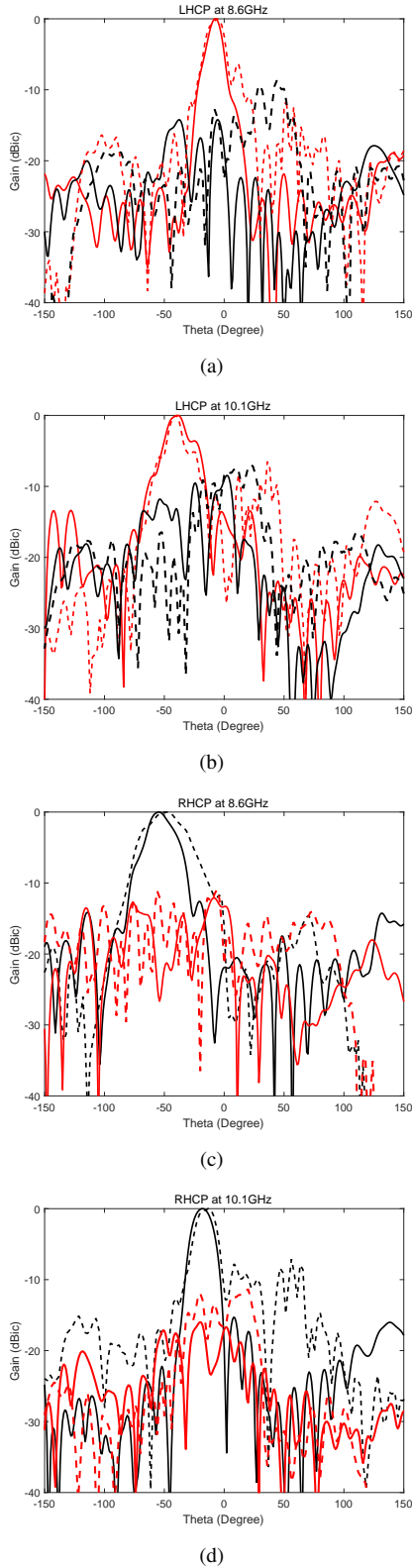


Fig. 14. Simulated and measured radiations patterns when Feed B is excited: (a) LHCP beams at 8.6GHz; (b) LHCP beams at 10.1GHz; (c) RHCP beams at 8.6GHz; (d) RHCP beams at 10.1GHz. (Black solid line: simulated RHCP, Black dashed line: measured RHCP, Red solid line: simulated LHCP, Red dashed line: measured LHCP)

oped reflectarray with one feed activated when placing it on the

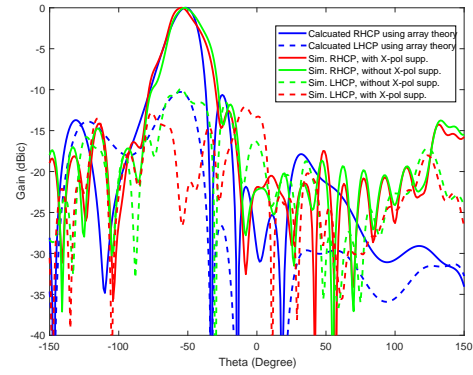


Fig. 15. Comparison of the simulated RHCP radiation pattern of the reflectarray at 8.6GHz with and without applying the cross polarization suppression technique, and the theoretical calculation.

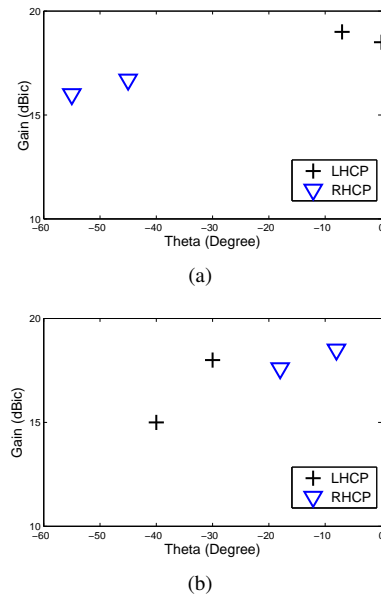


Fig. 16. Measured Gain variation of the present reflectarray at varied scan angles (a) 8.6GHz and (b) 10.1GHz.

roof of a real size car model. The simulation was performed by using Ansys Savant software to predict the performance of the developed reflectarray when it is installed on the car by using the ray tracing method. As shown, the roof of the car does not affect the radiation performance of the developed array antenna and at each frequency band, there are two directional beams. This is because most of the incident wave from the feed antenna is concentrated on the array aperture. It should be noted that the developed multibeam reflectarray can be scaled to achieve a higher gain by increasing the number of the antenna elements.

Table II compares the present design with other reported dual-CP reflectarrays. This table also includes some reflectarrays that can be extended to the dual-CP designs. The maximum beam scanning angle of some of these reported designs may possibly be increased but they were not explicitly described. Compared to these designs, the present design achieves dual-band and dual-CP operation with independent

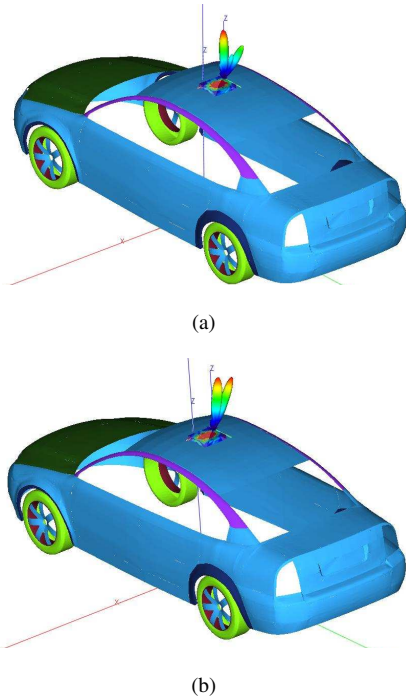


Fig. 17. Simulated radiation patterns (in linear scale) of the developed reflectarray when placing on the car roof (a) 8.6GHz and (b) 10.1GHz. Only one feed is activated in this simulation.

beam control using a single aperture. Meanwhile, the present design achieves the largest beam-scanning range with dual-CP radiation and low fabrication complexity.

TABLE II

COMPARISON OF THE PRESENT DESIGN WITH OTHER REPORTED DUAL-CP REFLECTARRAYS

	Dual-CP	Independent beam control	Max. beam angle	Remark
This work	Yes, simultaneously	Yes, at each frequency and polarization	$55^\circ$	dual-band, shared aperture
[19]	No	N.A	N.A	single band; can be extended to dual-CP with dual-surface
[20]	Yes, simultaneously	Yes, at each polarization	N.A	single band; dual-surface reflector
[21]	Yes, simultaneously	Yes, at each polarization	$21^\circ$	single-band; two apertures
[28]	No	N.A	$43^\circ$	linear direct radiating array
[29]	No	N.A	$20^\circ$	linear direct radiating array

## V. DISCUSSION

The present design has the potential to be further developed to continuous beam-steering reflectarrays by integrating the phase shifters (PS) to the antenna elements instead of using passive phase delay lines. This concept is shown in Fig. 18.

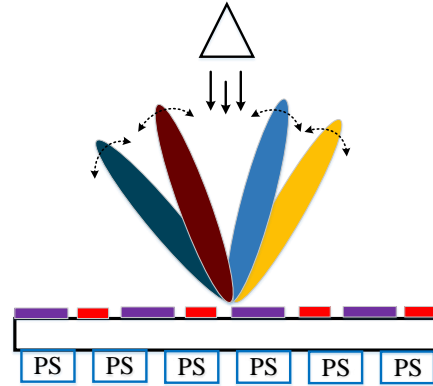


Fig. 18. The concept of continuously beam-steering by incorporating phase shifters to the present CP reflectarrays.

As shown, only one feed antenna is required and the four beams can be independently as well as continuously scanned within a large angle range. Besides using conventional phase shifters, recent research progress on the tunable materials such as electrically tunable barium strontium titanate perovskite (BSTO) films can also be applied to the array antenna design [30], [31], [32]. The thin films show high relative permittivity, low loss tangent, and high tunability, which can be used to develop BSTO based phase shifters. For example, the  $Mn$ -doped BSTO films presented in [30] show promising dielectric tunability and low insertion loss (3.2 dB at 10 GHz with the coplanar waveguides). The future development in materials is expected to make these tunable materials more suitable for Satcom-on-the-Move array antenna applications with moderate cost.

## VI. CONCLUSION

A multibeam dual-CP reflectarray for CAV application is presented in this paper. The reflectarray uses a single aperture and single feed to realize four simultaneous CP beams that can be independently controlled. Each of the beams corresponds to different frequencies and polarizations. A cross-polarization suppression technique is developed to improve the beam scanning angle of the CP reflectarray, which is validated by simulation, measurement and theoretical calculated results. The present antenna design concept is flexible and can be applied to the design of dual-band reflectarrays with different frequency ratios and directivity.

## REFERENCES

- [1] L. Guvenc, B. A. Guvenc, and M. T. Emirler, *Connected and Autonomous Vehicles*. Wiley-Blackwell, 2016, ch. 35, pp. 581–595.
- [2] P. Bansal and K. M. Kockelman, “Forecasting americans long-term adoption of connected and autonomous vehicle technologies,” *Transportation Research Part A: Policy and Practice*, vol. 95, pp. 49 – 63, 2017.
- [3] “Connected & autonomous vehicles,” The Satellite Applications Catalog, Tech. Rep., 2016.
- [4] “Market forecast for connected and autonomous vehicles,” Centre for Connected and Autonomous Vehicles, Tech. Rep., 2017.
- [5] J. B. Kenney, “Dedicated short-range communications (DSRC) standards in the united states,” *Proceedings of the IEEE*, vol. 99, no. 7, pp. 1162–1182, July 2011.

- [6] Y. Lin, P. Wang, and M. Ma, "Intelligent transportation system (ITS): Concept, challenge and opportunity," in *2017 IEEE 3rd international conference on big data security on cloud (bigdatasecurity), IEEE international conference on high performance and smart computing (hpsc), and IEEE international conference on intelligent data and security (ids)*, May 2017, pp. 167–172.
- [7] T. Varum, J. N. Matos, P. Pinho, and R. Abreu, "Nonuniform broadband circularly polarized antenna array for vehicular communications," *IEEE Transactions on Vehicular Technology*, vol. 65, no. 9, pp. 7219–7227, Sept 2016.
- [8] G. N. Alsath, H. Arun, Y. P. Selvam, M. Kanagasabai, S. Kingsly, S. Subbaraj, R. Sivasamy, S. K. Palaniswamy, and R. Natarajan, "An integrated tri-band/uwb polarization diversity antenna for vehicular networks," *IEEE Transactions on Vehicular Technology*, pp. 1–1, 2018.
- [9] Q. Wu, Y. Zhou, and S. Guo, "An l-sleeve l-monopole antenna fitting a shark-fin module for vehicular LTE, WLAN and car-to-car communications," *IEEE Transactions on Vehicular Technology*, pp. 1–1, 2018.
- [10] Y. B. Jung, S. Y. Eom, and S. I. Jeon, "Novel antenna system design for satellite mobile multimedia service," *IEEE Transactions on Vehicular Technology*, vol. 59, no. 9, pp. 4237–4247, Nov 2010.
- [11] Y. Q. Wen, B. Z. Wang, and X. Ding, "Wide-beam circularly-polarized microstrip magnetic-electric dipole antenna for wide-angle scanning phased array," *IEEE Antennas and Wireless Propagation Letters*, vol. PP, no. 99, pp. 1–1, 2016.
- [12] W. Menzel and D. Kessler, "A folded reflectarray antenna for 2d scanning," in *2009 German Microwave Conference*, March 2009, pp. 1–4.
- [13] J. Huang and J. A. Encinar, *Reflectarray Antennas*. Wiley-Blackwell, 2007.
- [14] Q. Luo, S. Gao, C. Zhang, D. Zhou, T. Chaloun, W. Menzel, V. Ziegler, and M. Sobhy, "Design and analysis of a reflectarray using slot antenna elements for ka-band satcom," *IEEE Transactions on Antennas and Propagation*, vol. 63, no. 4, pp. 1365–1374, April 2015.
- [15] T. Chaloun, V. Ziegler, and W. Menzel, "Design of a dual-polarized stacked patch antenna for wide-angle scanning reflectarrays," *IEEE Transactions on Antennas and Propagation*, vol. 64, no. 8, pp. 3380–3390, Aug 2016.
- [16] M. Li, S. Q. Xiao, and B. Z. Wang, "Investigation of using high impedance surfaces for wide-angle scanning arrays," *IEEE Transactions on Antennas and Propagation*, vol. 63, no. 7, pp. 2895–2901, July 2015.
- [17] Y. Lyu, F. Meng, G. Yang, D. Erni, Q. Wu, and K. Wu, "Periodic siw leaky-wave antenna with large circularly polarized beam scanning range," *IEEE Antennas and Wireless Propagation Letters*, vol. 16, pp. 2493–2496, 2017.
- [18] J. Huang and R. J. Pogorzelski, "A Ka-band microstrip reflectarray with elements having variable rotation angles," *IEEE Transactions on Antennas and Propagation*, vol. 46, no. 5, pp. 650–656, May 1998.
- [19] J. Sanz-Fernandez, E. Saenz, and P. de Maagt, "A circular polarization selective surface for space applications," *IEEE Transactions on Antennas and Propagation*, vol. 63, no. 6, pp. 2460–2470, June 2015.
- [20] M. A. Joyal, R. E. Hani, M. Riel, Y. Demers, and J. J. Laurin, "A reflectarray-based dual-surface reflector working in circular polarization," *IEEE Transactions on Antennas and Propagation*, vol. 63, no. 4, pp. 1306–1313, April 2015.
- [21] S. Mener, R. Gillard, R. Sauleau, A. Bellion, and P. Potier, "Dual circularly polarized reflectarray with independent control of polarizations," *IEEE Transactions on Antennas and Propagation*, vol. 63, no. 4, pp. 1877–1881, April 2015.
- [22] P. Pan, H. Wang, Z. Zhao, and W. Zhang, "How many antenna arrays are dense enough in massive mimo systems," *IEEE Transactions on Vehicular Technology*, vol. 67, no. 4, pp. 3042–3053, April 2018.
- [23] L. Yang, Y. Zeng, and R. Zhang, "Channel estimation for millimeter-wave MIMO communications with lens antenna arrays," *IEEE Transactions on Vehicular Technology*, vol. 67, no. 4, pp. 3239–3251, April 2018.
- [24] K.-F. Lee, K.-M. Luk, and J. Daele, "Characteristics of the equilateral triangular patch antenna," *Antennas and Propagation, IEEE Transactions on*, vol. 36, no. 11, pp. 1510–1518, Nov 1988.
- [25] I. J. Bahl and D. K. Trivedi, "A designer's guide to microstrip line," *Microwaves*, pp. 174–182, May 1997.
- [26] M. J. Franco, "A high-performance dual-mode feed horn for parabolic reflectors with a stepped-septum polarizer in a circular waveguide [antenna designer's notebook]," *IEEE Antennas and Propagation Magazine*, vol. 53, no. 3, pp. 142–146, June 2011.
- [27] Y. Mao, S. Xu, F. Yang, and A. Z. Elsherbeni, "A novel phase synthesis approach for wideband reflectarray design," *IEEE Transactions on Antennas and Propagation*, vol. 63, no. 9, pp. 4189–4193, Sept 2015.
- [28] C. Liu, S. Xiao, Y. X. Guo, Y. Y. Bai, and B. Z. Wang, "Broadband circularly polarized beam-steering antenna array," *IEEE Transactions on Antennas and Propagation*, vol. 61, no. 3, pp. 1475–1479, March 2013.
- [29] M. Maqsood, S. Gao, T. W. C. Brown, M. Unwin, R. de vos Van Steenwijk, J. D. Xu, and C. I. Underwood, "Low-cost dual-band circularly polarized switched-beam array for global navigation satellite system," *IEEE Transactions on Antennas and Propagation*, vol. 62, no. 4, pp. 1975–1982, April 2014.
- [30] I. Bakaimi, X. He, S. Guerin, N. Hashim, Q. Luo, I. Reaney, S. Gao, K. Groot, and B. Hayden, "Combinatorial synthesis and screening of (ba,sr)(ti,mn)o3 thin films for optimization of tunable co-planar waveguides," *J. Mater. Chem. C*, pp. –, 2018.
- [31] H. V. Nguyen, R. Benzerga, C. Borderon, C. Delaveaud, A. Sharaiha, R. Renoud, C. Paven, S. Pavy, K. Nadaud, and H. W. Gundel, "Miniaturized and reconfigurable notch antenna based on a bst ferroelectric thin film," *Materials Research Bulletin*, vol. 67, pp. 255 – 260, 2015.
- [32] K. K. Karnati, Y. Shen, M. E. Trampler, S. Ebadi, P. F. Wahid, and X. Gong, "A bst-integrated capacitively loaded patch for  $K_a$ - and  $X$ -band beamsteerable reflectarray antennas in satellite communications," *IEEE Transactions on Antennas and Propagation*, vol. 63, no. 4, pp. 1324–1333, April 2015.



**Qi Luo (S'08–M'12)** was born in Chengdu, China in 1982. He received his MSc degree from university of Sheffield, UK in 2006 and his Ph.D. degree from University of Porto, Portugal in 2012. From 2012–2013, he worked at Surrey space centre, UK as a research fellow. Currently, he is working at School of Engineering and Digital Arts, University of Kent, UK as a research fellow. His research interests include smart antennas, circularly polarized antennas, reflectarray, multiband microstrip antennas and electrically small antenna design. He authored/co-



authored two books *Circularly Polarized Antennas* (Wiley-IEEE, 2014) and *Low-Cost Smart Antennas* (Wiley, 2019). He has been serving as a reviewer for a number of technical journals and international conferences.

**Steven Gao (M'01–SM'16–F'19)** received the PhD from Shanghai University, P.R. China. He is a Professor and Chair of RF and Microwave Engineering, and the Director of Postgraduate Research at School of Engineering and Digital Arts, University of Kent, UK. His research interests include smart antenna, phased array, MIMO, broadband and multi-band antennas, small antennas, RF front ends, FSS, and their applications into 5G mobile communications, satellite communication, small satellites, radars, energy harvesting and medical systems. He co-edited/co-authored 3 books including *Space Antenna Handbook* (Wiley, 2012), *Circularly Polarized Antennas* (Wiley-IEEE, 2014), *Low-Cost Smart Antennas* (Wiley, 2019), over 300 papers and 8 patents. He received the 2016 IET Premium Award for the Best Paper in IET Microwave, Antennas and Propagation, the 2017 CST University Publication Award for a paper in *IEEE Transactions on Antennas and Propagation*, etc. He was a Distinguished Lecturer of IEEE Antennas and Propagation Society, and is an Associate Editor of several Journals (*IEEE Transactions on Antennas and Propagation*, *Radio Science*, *Electronics Letters*, *IEEE Access*, *IET Circuits, Devices and Systems*, etc), the Editor-in-Chief for Wiley Book Series on "Microwave and Wireless Technologies", and an editorial board member of many international Journals. He was the General Chair of 2013 Loughborough Antenna and Propagation Conference, Guest Editor of Proceedings of the IEEE for Special Issue on Small Satellites (March 2018), Guest Editor of *IEEE Trans on Antennas and Propagation* for Special Issue on "Antennas for Satellite Communication" (2015), and Guest Editor of *IET Circuits, Devices & Systems* for Special Issue in Photonic and RF Communications Systems (2014). He was an invited speaker in many international conferences. He is a Fellow of IEEE, the Royal Aeronautical Society, and the IET.



**Wenting Li** received the B.S. degree in electronic information engineering and the M.S. degree in electromagnetic field and microwave technology from Northwestern Polytechnical University, Xian, China, in 2011 and 2014, respectively. He is currently pursuing the Ph.D. degree with the University of Kent, Canterbury, U.K. His current research interests include reflectarray antennas, reconfigurable antennas, circularly polarized antennas, and multibeam antennas.



**Mohammed Sobhy (LM'90)** received the B.Sc. degree in electrical engineering from the University of Cairo, Cairo, Egypt, in 1956, and the Ph.D. degree from the University of Leeds, Leeds, U.K., in 1966. He is an Emeritus Professor of Electronics with the University of Kent, Canterbury, U.K. His current research interests include analysis and applications of nonlinear electronic systems.



**Ioanna Bakaimi** is a Research Fellow in the Advanced Composite Materials Group at the Chemistry Department University of Southampton. She obtained her PhD in 2015 from the Functional Nanocrystals and Quantum Magnetism Laboratory at the IESL-FORTH and the Department of Physics, University of Crete, Greece. Her expertise is focused in the interatomic interactions of solid state systems and specifically in the interplay of the crystal structure with the physical properties and functionalization of magnetic, dielectric and ferroelectric

oxides. She has also been a guest researcher in the Neutron Centre of National Institute of Standards and Technology (NCNR-NIST, USA) where she carried out Neutron Diffraction experiments as well as crystal and magnetic structure analysis. Since 2016 she is a Research Fellow in the Advanced Composite Materials Group at the Chemistry Department, University of Southampton. Her work focuses on the optimization of lead niobate pyrochlore tunable dielectric thin films for high frequency applications.



**CH Kees de Groot (M'00–SM'05)** received a Master's degree in Physics in 1994 from the University of Groningen, the Netherlands, and a Ph.D. degree in 1998 from the University of Amsterdam for research carried out at the Philips Research laboratories in Eindhoven. Subsequently, he was a Research Fellow at the Massachusetts Institute of Technology (MIT), Cambridge, U.S. where he conducted research on spin tunnel junction and phase change materials. Since 2000 he is with the department of Electronics and Computer Science of the University of

Southampton, U.K., where he is a full Professor since 2012. His main interest is the integration of novel nano-materials and devices with silicon electronics processing with particular emphasis on the semiconducting and dielectric properties of oxides, chalcogenides, and carbides. His recent breakthroughs in these areas includes the first 100 nm GeSbTe phase change memory by non-aqueous electrodeposition, SiC resistive memory with a record 9 orders of magnitude on/off ratio, and functional oxide nanostructures resulting in plasmonic devices with ultrafast modulation of optical and dielectric properties of ITO, AZO and VO<sub>2</sub> by optical, electrical, and thermal methods. He is an author of over 125 journal publications.



**CH Kees de Groot (Brian Hayden)** obtained his PhD in Bristol in 1979 in Surface Science, and continued this work as a postdoctoral fellow at the Fritz Haber Institute of the Max Planck Society, Berlin. Appointed lecturer at the University of Bath he developed supersonic molecular beam techniques to study reaction dynamics at single crystal metal surfaces. He was appointed lecturer at the University of Southampton in 1988, working in the fields of surface science and catalysis and electro-catalysis, and was appointed to a Personal Chair in 1995. In

2000, he extended thin film MBE based methodologies to the combinatorial synthesis and screening of solid state materials and catalysts. He is a founder (2004), an executive director and Chief Scientific Officer of Ilika plc (AIM 2010 in the Guardian/Library House Clean Tech 100), a 50M spin-out company involved in materials discovery and development for the electronics and energy sectors, and with strong partnerships with multinational corporations in these sectors. He recently founded and directs the Advanced Composite Materials Laboratory at the University of Southampton, extending materials development into new areas of application, and their incorporation into devices, by applying evaporative PVD methods in a 150mm wafer based cluster production tool. His present research interests include the continued development of fuel cell electrocatalysts, materials in solid state lithium ion batteries, phase change and resistive memory materials, thermoelectric and optoelectronic materials, metamaterials and tunable dielectric materials. He is author of over 150 refereed papers h-index 39 and over 30 active patent families including new catalysts and materials for low temperature fuel cells and solid state Li-ion batteries. He is a Fellow of the Royal Society of Chemistry and Fellow of the Institute of Physics.



**Ian Reaney** is the Director of Research and Innovation at the Department of Materials Science and Engineering. He was awarded a Personal Chair at University of Sheffield in 2007 and is now the Dyson Chair in Ceramics. He joined the Faculty of Engineering in 1994, initially as a PDRA, then as a Lecturer from 1995. He obtained his PhD from the University of Manchester in 1989 and worked as post-doctoral researcher at the University of Essex before joining the Laboratoire de Ceramique, Ecole Polytechnique Federale de Lausanne in Switzerland

in 1991. The main theme of Prof. Reaney's research is the study of structure/microstructure property relations in electroceramics.



**Xuexia Yang (M'05–SM'17)** received the B.S. and M.S. degrees from Lanzhou University, Lanzhou, China, in 1991 and 1994, respectively, and the Ph.D. degree in electromagnetic field and microwave technology from Shanghai University, Shanghai, China, in 2001. From 1994 to 1998, she was a teaching assistant and a lecturer in Lanzhou University, China. From 2001 to 2008, she was a lecture and an associate professor in Shanghai University, China. She is currently a professor and the Head of the Antennas and Microwave R&D Center at Shanghai

University. She has authored or co-authored over 180 technical journal and conference papers. She is also a frequent reviewer for over 10 scientific journals. Her research interests include antennas theory and technology, computational electromagnetic and microwave power transmission. She is now a member of the Committee of Antenna Society of China Electronics Institute and Senior Member of China Electronics Institute. She is an associate editor for the Journal of Shanghai University (Science edition).